



Published in final edited form as:

Amino Acids. 2019 March ; 51(3): 513–528. doi:10.1007/s00726-018-02687-x.

Altered brain arginine metabolism in a mouse model of tauopathy

Pranav Vemula^{1,3}, Yu Jing^{1,3}, Hu Zhang^{2,3}, Jerry B. Hunt Jr.⁴, Leslie A. Sandusky–Beltran⁴, Daniel C. Lee⁴, and Ping Liu^{1,2,3}

¹Department of Anatomy, School of Biomedical Sciences, Brain Health Research Centre, University of Otago, Dunedin, New Zealand ²School of Pharmacy, Brain Health Research Centre, University of Otago, Dunedin, New Zealand ³Brain Research New Zealand, Dunedin, New Zealand ⁴Byrd Alzheimer's Institute, College of Pharmacy and Pharmaceutical Sciences, University of South Florida, Florida, USA

Abstract

Tauopathies consist of intracellular accumulation of hyperphosphorylated and aggregated microtubule protein tau, which remains a histopathological feature of Alzheimer's disease (AD) and frontotemporal dementia. L-Arginine is a semi-essential amino acid with a number of bioactive molecules. Its downstream metabolites putrescine, spermidine, and spermine (polyamines) are critically involved in microtubule assembly and stabilization. Recent evidence implicates altered arginine metabolism in the pathogenesis of AD. Using high-performance liquid chromatographic and mass spectrometric assays, the present study systematically determined the tissue concentrations of L-arginine and its nine downstream metabolites in the frontal cortex, hippocampus, parahippocampal region, striatum, thalamus, and cerebellum in male PS19 mice-bearing human tau P301S mutation at 4, 8, and 12–14 months of age. As compared to their wild-type littermates, PS19 mice displayed early and/or prolonged increases in L-ornithine and altered polyamine levels with age. There were also genotype- and age-related changes in L-arginine, L-citrulline, glutamine, glutamate, and γ -aminobutyric acid in a region-and/or chemical-specific manner. The results demonstrate altered brain arginine metabolism in PS19 mice with the most striking changes in L-ornithine, polyamines, and glutamate, indicating a shift of L-arginine metabolism to favor the arginase–polyamine pathway. Given the role of polyamines in maintaining microtubule stability, the functional significance of these changes remains to be explored in future research.

Ping Liu, ping.liu@otago.ac.nz; Pranav Vemula, pranav.vemula@anatomy.otago.ac.nz; Yu Jing, rena.jing@anatomy.otago.ac.nz; Hu Zhang, hu.zhang@otago.ac.nz; Jerry B. Hunt Jr., jhunt2@health.usf.edu; Leslie A. Sandusky–Beltran, lesliesandusky@health.usf.edu; Daniel C. Lee, dlee1@health.usf.edu.

Conflict of interest The authors declare that they have no conflict of interest.

Ethical approval All procedures performed in studies involving animals were in accordance with the ethical standards of the institution.

Publisher's Note Springer Nature remains neutral with regard to jurisdictional claims in published maps and institutional affiliations.

Keywords

Tauopathy; Arginine metabolism; L-Ornithine; Polyamines; Glutamate; Hippocampus

Introduction

Tauopathies consist of intracellular accumulation of hyperphosphorylated and aggregated microtubule protein tau. Abnormal tau deposits remain a prominent histopathological feature for several neurodegenerative disorders, such as Alzheimer's disease (AD) and frontotemporal dementia (FTD). AD is characterized behaviorally by progressive memory loss in aged individuals with the presence of extracellular amyloid plaques in the affected brain regions (Castellani et al. 2010). FTD often affects individuals younger than 65 years with frontotemporal lobar degeneration (Cairns et al. 2007). It has been shown that multiple pathogenic mutations in microtubule-associated protein tau (MAPT) are associated with diverse FTD syndromes, indicating the specific contribution of tau abnormalities to frontotemporal lobar degeneration (Irwin et al. 2015). Experimentally, transgenic mouse lines bearing the MAPT P301 mutation have been used to mimic human frontotemporal lobar degeneration (Yoshiyama et al. 2007; López-González et al. 2015).

L-Arginine is a semi-essential amino acid that can be metabolized enzymatically to produce several bioactive molecules (Wu and Morris 1998; Fig. 1). Nitric oxide synthase (NOS), for example, converts L-arginine to L-citrulline and a gaseous molecule nitric oxide (NO). In the brain, NO derived from neuronal and endothelial NOS (nNOS and eNOS, respectively) is vital for synaptic plasticity, learning, and memory, and has an important role in maintaining cerebral blood flow (Esplugues 2002). Excessive production of NO derived from inducible NOS (iNOS), however, can lead to neurotoxicity and neurodegeneration (Calabrese et al. 2007). Arginase (arginases I and II) metabolizes L-arginine to form L-ornithine with urea as a by-product. L-ornithine is further metabolized by ornithine decarboxylase (ODC) to produce putrescine, but can also be channelled to produce glutamate, glutamine and γ -aminobutyric acid (GABA) (Wu and Morris 1998). It has been well documented that physiological concentrations of polyamines (putrescine, spermidine, and spermine) are essential in maintaining normal cellular function (Williams 1997; Wu and Morris 1998; Wallace et al. 2003; Bae et al. 2018). Arginine decarboxylase (ADC) converts L-arginine to agmatine, which is further metabolized by agmatinase to form putrescine. Li et al. (1994) first reported the presence of agmatine and its biosynthetic enzyme ADC in the brain. Endogenous agmatine has been considered a novel putative neurotransmitter (for reviews, see Reis and Regunathan 2000; Piletz et al. 2013). Recent research has demonstrated learning-induced increases in agmatine in memory-related brain structures at the gross tissue, synaptic terminal, and extracellular levels (Liu et al. 2008, 2009; Leitch et al. 2011; Seo et al. 2011; Rushaidhi et al. 2013), suggesting the involvement of endogenous agmatine in learning and memory processes. Moreover, agmatine has an important role in regulating the production of NO and polyamines via its influences on NOS and ODC (Piletz et al. 2013).

Recent human post-mortem brain tissue research has shown altered arginine metabolism in AD brains. In the study of Liu et al. (2014), for example, there were markedly increased total arginase activity and arginase II protein expression, but dramatically decreased total NOS activity, nNOS and eNOS expression, reduced L-ornithine, agmatine and polyamine levels, and intensively labelled iNOS-immunoreactive neurons and astrocytic clusters in the AD hippocampus and superior frontal gyrus, the brain structures that are affected severely by the disease. Inoue et al. (2013), however, found increased polyamine levels in the AD frontal and occipital lobes. It is currently unclear whether the differences in race (Caucasian vs Asian), age and/or brain region examined contribute to the discrepancy in polyamine data between the two studies. Nevertheless, the existing human tissue work suggests the potential contribution of altered arginine metabolism to the neuropathology and cognitive impairments in AD.

To date, very little if any data show how arginine metabolism changes in the brain of FTD patients. Using rTg4510 mice bearing the human tau P301L mutation, Hunt et al. (2015a) demonstrated that sustained arginase I overexpression over a 4-month period from the beginning of brain tau deposition markedly reduced tau pathology and several kinases capable of phosphorylating tau and mitigated hippocampal atrophy in this mouse model of forebrain tauopathy. It has been shown that polyamines are critically involved in microtubule assembly and stabilization (Savarin et al. 2010 ; Hamon et al. 2011; Song et al. 2013), and the high-order polyamine spermine increases the acetylation of microtubules and facilitates autophagic degradation of prion aggregates (Phadwal et al. 2018). Moreover, our recent preliminary work demonstrated that polyamines (spermine in particular) decreased tau aggregation and promoted micro-tubule assembly (Hunt et al. 2015b). The findings of Hunt et al. (2015a), therefore, suggest that the arginase–polyamine system might be affected in tauopathies and shifting L-arginine metabolism to favor the polyamine pathway might curtail tau pathology, which may explain the beneficial effects of arginase I overexpression (hence increased polyamine production). However, it is currently unknown how brain arginine metabolism changes in mice bearing the human tau P301 mutation.

PS19 mice express P301S mutant tau, and have been used to model human frontotemporal lobar degeneration (López-González et al. 2015). These mice display filamentous tau lesions at 6 months of age, and show striking neuronal loss and cortical and hippocampal atrophy at 9–12 months of age (Yoshiyama et al. 2007). Remarkably, synapse loss and synaptic dysfunction in the hippocampus are evident in PS19 mice at 3 months of age, even prior to the formation of fibrillary tau tangles (Yoshiyama et al. 2007). Given the role of polyamines in maintaining microtubule stability and degrading protein aggregates (Savarin et al. 2010; Hamon et al. 2011; Song et al. 2013; Phadwal et al. 2018), we hypothesized that this could be due, in part, to alterations in brain arginine metabolism (polyamines in particular) in PS19 mice. To test this hypothesis, the present study systematically determined the time course of the arginine metabolic profile changes in the frontal cortex, hippocampus, parahippocampal region, striatum, thalamus, and cerebellum of PS19 mice at 4, 8, and 12–14 months of age.

Materials and methods

Animals

The present study used male P301S tau transgenic (PS19) mice [B6;C3-Tg(Prnp-MAPT*P301S)PS19Vle/J; stock number: 008169] that expressed the P301S mutant form of human microtubule-associated protein tau and their sex-matched wild-type littermates at 4 ($n = 8/\text{genotype}$), 8 ($n = 8/\text{genotype}$), and 12–14 (WT: $n = 11$, PS19: $n = 8$) months of age. The reason for using the males only in the present study was because male PS19 mice develop tau pathology more consistently and robustly relative to the females based on information from the Jackson Laboratory and earlier research (Zhang et al. 2012; Sankaranarayanan et al. 2015). All animals were housed individually, maintained on a 12-h light/dark cycle (lights on at 6 AM), and provided ad libitum access to food and water. All experimental procedures were carried out in accordance with the regulations of the University of South Florida (IACUC #1594).

Tissue collection

All animals were weighed, anesthetized with barbiturates, and transcardially perfused with 25 ml of 0.9% saline. The saline perfused unfixed brain from each animal was rapidly removed and transferred to cold saline. The frontal cortex, whole hippocampus, parahippocampal region (containing the entorhinal, perirhinal, and postrhinal cortices), striatum, thalamus, and cerebellum were then dissected freshly on ice from each hemisphere. Procedures for the tissue dissections were based on the studies of Hortnagl et al. (1991), Burwell (2001) and Bergin et al. (2018). The brain tissue samples were snap-frozen and stored at $-80\text{ }^{\circ}\text{C}$, and then freighted (on dry ice) from the University of South Florida, USA to the University of Otago, New Zealand.

Neurochemical procedures

All the snap-frozen samples were weighed, homogenized in ice-cold 10% perchloric acid ($\sim 50\text{ mg wet weight per ml}$), and centrifuged at $10,000\text{ g}$ for 10 min to precipitate protein (Bergin et al. 2018). The perchloric acid extracts (supernatants) were then stored at $-80\text{ }^{\circ}\text{C}$ until the high-performance liquid chromatography (HPLC) and liquid chromatography/mass spectrometric (LC/MS) assays.

The concentrations of L-arginine, L-citrulline, L-ornithine, glutamine, glutamate, GABA, spermidine, and spermine in each brain region were measured using the HPLC method, whereas the agmatine and putrescine levels were determined by a highly sensitive LC/MS/MS method, as detailed in our previous publications (Gupta et al. 2012; Liu et al. 2014, 2016; Bergin et al. 2018). High-purity external and internal standards (Sigma, Sydney, Australia) were used and all other chemicals were of analytical grade. For each brain region, the samples from both the WT and PS19 groups at all three age points were assayed at the same time in a counterbalanced manner, and the assays were performed in duplicate. The concentrations of L-arginine and its downstream metabolites in the brain tissue were calculated with reference to the peak area of external standards, and values were expressed as $\mu\text{g/g}$ wet tissue (Gupta et al. 2012; Liu et al. 2014, 2016; Bergin et al. 2018).

Experimenters were blind to the grouping information during the tissue preparation and assays.

Statistical analysis

Neurochemical data were analyzed using two-way analysis of variance (ANOVA) followed by Bonferroni post-hoc tests, as the samples from all three age groups were assayed at the same time. Statistical analysis was performed using Graphpad Prism software, and all data were presented as mean \pm SEM. The level of significance was set at $p < 0.05$ for all comparisons (Zolman 1993).

Results

Both HPLC and LC/MS assays were used to quantify the tissue concentrations of l-arginine and its downstream metabolites (L-citrulline, L-ornithine, glutamine, glutamate, GABA, agmatine, putrescine, spermidine, and spermine) in the frontal cortex, hippocampus, parahippocampal region, striatum, thalamus, and cerebellum obtained from both the WT and PS19 mice at 4, 8, and 12–14 months of age.

Frontal cortex

For L-arginine (Fig. 2a) and L-citrulline (Fig. 2b), two-way ANOVA revealed a significant genotype \times age interaction (L-arginine: $F(2,45) = 3.31$, $p = 0.046$; L-citrulline: $F(2,45) = 4.85$, $p = 0.013$), but no effect of genotype (all $F < 1$) or age (L-arginine: $F(2,45) = 2.59$, $p = 0.086$; L-citrulline: $F(2,45) = 2.42$, $p = 0.11$). For L-ornithine (Fig. 2c), interestingly, there was a highly significant effect of genotype [$F(1,45) = 20.59$, $p < 0.0001$], but no effect of age [$F(2,45) = 2.28$, $p = 0.11$] or genotype \times age interaction ($F < 1$), with higher levels in PS19 mice relative to the WT mice at all three ages (approximately 35–40% increase; all $p < 0.05$). For glutamine (Fig. 2d), there was no effect of genotype, age or genotype \times age interaction (all $F < 1$). For glutamate (Fig. 2e), there were significant effects of genotype [$F(1,45) = 4.21$, $p = 0.046$], age [$F(2,45) = 9.21$, $p = 0.0005$], and genotype \times age interaction [$F(2,45) = 4.41$, $p = 0.018$], with lower levels in PS19 mice at 8 and 12–14 months of age relative to their age-matched WT mice (about 10–15% decrease; all $p < 0.05$). When the glutamine and glutamate ratio was analyzed (Fig. 2g), there was no significant effect of genotype ($F < 1$), age ($F < 1$), or genotype \times age interaction [$F(2,45) = 2.93$, $p = 0.064$]. However, a planned comparison revealed a higher glutamine/glutamate ratio in PS19 mice relative to WT mice at 12–14 months of age (20% increase; $p < 0.001$). Regarding GABA (Fig. 2f) and glutamate/GABA ratio (Fig. 2h), there were significant effects of age [GABA: $F(2,45) = 5.75$, $p = 0.006$; glutamate/GABA ratio: $F(2,45) = 7.55$, $p = 0.0015$], but not genotype or genotype \times age interaction (all $F < 1$), with a trend of lower GABA level or higher glutamate/GABA ratio in 8-month WT and PS19 mice. For agmatine (Fig. 2i) and spermidine (Fig. 2k), we found significant effects of age [agmatine: $F(2,45) = 3.66$, $p = 0.034$; spermidine: $F(2,45) = 4.81$, $p = 0.0013$], but not genotype or genotype \times age interaction (all $F < 1$), with a trend of lower agmatine levels in 8-month WT and PS19 mice and increased spermidine levels with age in both groups. When putrescine was analysed (Fig. 2j), there were significant effects of genotype [$F(1,45) = 5.56$, $p = 0.023$], age [$F(2,45) = 12$, $p < 0.0001$], and genotype \times age interaction [$F(2,45) = 18.78$, $p < 0.0001$], with PS19

mice showing reduced (40% decrease; $p < 0.05$), but increased (135% increase; $p < 0.001$), putrescine levels at 4 and 12–14 months of age, respectively. For spermine (Fig. 2l), we observed a significant effect of genotype [$F(1,45) = 5.09, p = 0.029$], but no age effect or genotype \times age interaction (all $F < 1$), with a trend of lower levels in the PS19 group at all three ages.

Hippocampus

Regarding L-arginine (Fig. 3a), there were significant effects of genotype [$F(1,45) = 20.79, p < 0.0001$] and genotype \times age interaction [$F(2,45) = 5.57, p = 0.007$], but no age effect [$F(2,45) = 2.09, p = 0.14$], with higher levels in 12–14-month-old PS19 mice relative to their age-matched WT mice (48% increase; $p < 0.0001$). For L-citrulline (Fig. 3b), we observed a significant effect of age [$F(2,45) = 4.17, p = 0.022$], but no genotype effect or genotype \times age interaction (all $F = 1$), with a trend of reduced levels with age in both genotype groups. For L-ornithine (Fig. 3c), two-way ANOVA revealed significant effects of genotype [$F(1,45) = 26.13, p < 0.0001$] and age [$F(2,45) = 6.92, p = 0.0024$], as well as their interaction [$F(2,45) = 3.31, p = 0.046$], with higher levels in PS19 mice at 4 (16% increase; $p = 0.05$), 8 (37% increase; $p < 0.01$), and 12–14 (58% increase; $p < 0.001$) months of age. There were no effects of genotype and age, as well as their interaction, in glutamine (all $F < 1$; Fig. 3d). For glutamate (Fig. 3e), we found significant effects of age [$F(2,45) = 15.93, p < 0.0001$] and genotype \times age interaction [$F(2,45) = 5.61, p = 0.0069$], but no genotype effect ($F = 1$), with over-all reduced levels with age in both genotype groups, and higher and lower levels in 4- (20% increase; $p < 0.05$) and 12–14 (about 30% decrease; $p < 0.05$)-month PS19 mice, respectively, when compared to their age-matched WT controls. As for GABA (Fig. 3f), there was a significant effect of age [$F(2,45) = 7.11, p = 0.002$], but no genotype effect or genotype \times age interaction (all $F = 1$), with a trend of reduced levels with age in both genotype groups. When the glutamine/glutamate ratio was analysed (Fig. 3g), we observed significant effects of genotype [$F(1,45) = 8.22, p = 0.006$] and age [$F(2,45) = 15.89, p < 0.0001$] and their interaction [$F(2,45) = 11.02, p < 0.0001$], with markedly increased levels in 12–14-month-old PS19 mice relative to their age-matched WT mice (30% increase; $p < 0.0001$). Regarding the glutamate/GABA ratio (Fig. 3h), there were significant effects of age [$F(2,45) = 27.59, p < 0.0001$] and genotype \times age interaction [$F(2,45) = 7.41, p = 0.0017$], but no genotype effect ($F < 1$), with higher and lower levels in 4- (16% increase; $p < 0.05$) and 12–14 (26% decrease; $p < 0.01$)-month PS19 mice, respectively, when compared to their age-matched WT controls. For agmatine (Fig. 3i), there was a significant effect of age [$F(2,45) = 6.68, p = 0.029$], but no effect of genotype [$F(1,45) = 31.12, p = 0.084$] or genotype \times age interaction [$F(2,45) = 1.38, p = 0.26$], with an overall reduction with age in both genotype groups. When putrescine was analysed (Fig. 3j), we found significant effects of genotype [$F(1,45) = 25.65, p < 0.0001$] and age [$F(2,45) = 25.42, p < 0.0001$] and their interaction [$F(2,45) = 14.07, p < 0.0001$], with higher levels in PS19 mice at 8 (76% increase; $p = 0.05$) and 12–14 (208% increase; $p < 0.0001$) months of age relative to their age-matched WT mice. For spermidine (Fig. 3k), there were significant effects of genotype [$F(1,45) = 6.81, p = 0.012$] and age [$F(2,45) = 26.39, p < 0.0001$] and their interaction [$F(2,45) = 4.85, p = 0.012$], with higher levels in 12–14-month PS19 mice (39% increase; $p < 0.05$) relative to their age-matched controls. Regarding spermine (Fig. 3l), we observed significant effects of genotype [$F(1,45) = 7.68, p = 0.008$] and age [$F(2,45) = 7.43, p =$

0.0018], but no interaction ($F = 1$), with a trend of lower levels in 8- (22% decrease) and 12–14 (18% decrease)-month-old PS19 mice.

Parahippocampal region

For L-arginine (Fig. 4a), there was a significant genotype effect [$F(1,45) = 5.03, p = 0.03$], but no age effect or genotype x age interaction (all $F < 1$), with a trend of higher levels in PS19 mice at 4 and 12–14 months of age relative to their age-matched controls. For L-citrulline (Fig. 4b), we observed a significant genotype effect [$F(1,45) = 8.81, p = 0.0048$] and genotype \times age interaction [$F(2,45) = 15.03, p < 0.0001$], but no age effect [$F(2,45) = 2.07, p = 0.14$], with lower levels in 12–14-month-old PS19 mice when compared to the age-matched WT mice (30% decrease; $p < 0.0001$). Regarding L-ornithine (Fig. 4c), there were significant effects of genotype [$F(1,45) = 21.43, p < 0.0001$] and age [$F(2,45) = 3.96, p = 0.026$], but no genotype x age interaction ($F < 1$), with higher levels in 4-(30% increase), 8- (all $p < 0.01$), and 12–14 ($p < 0.05$)-month-old PS19 mice relative to their age-matched WT mice. For glutamine (Fig. 4d), there was no effect of genotype [$F(1,45) = 3.31, p = 0.075$], age ($F < 1$) or genotype x age interaction ($F < 1$). For glu-tamate (Fig. 4e), we found significant effects of genotype [$F(1,45) = 21.17, p < 0.0001$], age [$F(2,45) = 4.85, p = 0.0012$], and genotype \times age interaction [$F(2,45) = 12.53, p < 0.0001$], with lower levels in PS19 mice at 8 (10% decrease; $p < 0.05$) and 12–14 (25% decrease; $p < 0.0001$) months of age. Regarding GABA (Fig. 4f) and glutamine/glutamate ratio (Fig. 4g), there were no effects of genotype, age, and genotype \times age interaction (all $F = 1$). When the glutamate/GABA ratio was analysed (Fig. 4h), we observed significant effects of age [$F(2,45) = 5.62, p = 0.0066$], but not genotype [$F(2,45) = 3.18, p = 0.08$] or genotype \times age interaction ($F = 1$). There were no significant effects of genotype, age, and genotype \times age interaction (all $F = 1$) in agmatine (Fig. 4i) and spermidine (Fig. 4k). When putrescine was analysed (Fig. 4j), we found significant effects of genotype [$F(1,45) = 11.72, p = 0.0013$], age [$F(2,45) = 15.89, p < 0.0001$], and genotype x age interaction [$F(2,45) = 5.53, p = 0.007$], with higher levels in 8-(63% increase; $p = 0.05$) and 12–14 (76% increase; $p < 0.01$)-month-old PS19 mice relative to their age-matched WT mice. Regarding spermine (Fig. 4l), there were no significant effects of genotype [$F(1,45) = 3.39, p = 0.072$], age ($F < 1$), and genotype x age interaction [$F(1,45) = 2.86, p = 0.068$]. A planned comparison, however, indicated markedly reduced spermine levels in 12–14-month-old PS19 mice relative to their age-matched WT mice (24% decrease; $p < 0.01$).

Striatum

We found no effects of genotype, age, and their interaction in L-arginine (Fig. 5a), glutamine (Fig. 5d), GABA (Fig. 5f), spermidine (Fig. 5k), and spermine (Fig. 5l) (all $F = 1$). For L-citrulline (Fig. 5b), there was a significant genotype x age interaction [$F(2,45) = 4.54, p = 0.016$], but no effect of genotype or age (all $F = 1$). Post-hoc test indicated a lower level of L-citrulline in 12–14-month PS19 mice relative to controls (18% decrease; $p < 0.05$). Regarding L-ornithine (Fig. 5c), we observed a significant genotype effect [$F(1,45) = 5.97, p = 0.018$], but no age effect [$F(2,45) = 2.92, p = 0.065$] or genotype \times age interaction ($F < 1$), with higher levels in 4-month PS19 mice when compared to their age-matched controls (27% increase; $p < 0.01$). For glutamate (Fig. 5e), there was a significant genotype \times age interaction [$F(2,45) = 6.35, p = 0.0037$], but no effect of genotype [$F(1,45) = 2.90, p =$

0.095] or age ($F = 1$), with lower levels in 12–14-month PS19 mice relative to controls (18% decrease; $p < 0.01$). Regarding the glutamine/glutamate ratio (Fig. 5g), we found a significant genotype \times age interaction [$F(2,45) = 3.21, p = 0.049$], but no genotype, or age effect (all $F = 1$), with a higher value in 12–14-month PS19 mice (21% increase; $p < 0.01$). For the glutamate/GABA ratio (Fig. 5h), there was a significant effect of genotype [$F(2,45) = 7.19, p = 0.01$], but no age effect ($F = 1$) or genotype \times age interaction [$F(2,45) = 2.59, p = 0.086$], with a lower value in 12–14-month PS19 mice when compared to their age-matched WT controls (19% decrease; $p < 0.05$). Regarding agmatine (Fig. 5i), we observed a significant effect of age [$F(2,45) = 8.40, p = 0.0008$], but no genotype effect or its reaction with age (all $F = 1$), with a trend of age-related reduction in both genotypes. When putrescine was analysed (Fig. 5j), there were significant effects of genotype [$F(1,45) = 8.91, p = 0.0046$] and age [$F(2,45) = 25.56, p < 0.0001$], but no interaction ($F < 1$), with higher levels in PS19 mice at 4 (29% increase) and 12–14 (31% increase) months of age relative to their age-matched WT controls (all $p < 0.05$).

Thalamus

There were no effects of genotype and age and their interaction in L-arginine (Fig. 6a), L-citrulline (Fig. 6b), L-ornithine (Fig. 6c), glutamine (Fig. 6d), glutamate (Fig. 6e), glutamine/glutamate ratio (Fig. 6g), glutamate/GABA ratio (Fig. 6h), agmatine (Fig. 6i), and spermidine (Fig. 6k). For GABA (Fig. 6f), we observed a significant genotype \times age interaction [$F(2,45) = 3.50, p = 0.038$], but no genotype or age effect (all $F = 1$). When putrescine was analysed (Fig. 6j), there were significant effects of genotype [$F(1,45) = 5.40, p = 0.025$] and age [$F(2,45) = 13.53, p < 0.0001$] and their interaction [$F(2,45) = 6.74, p = 0.0028$], with higher levels in PS19 mice at 8 (37% increase) and 12–14 (51% increase) months of age relative to their age-matched WT controls (all $p < 0.05$). Regarding spermine (Fig. 6l), we found a significant genotype \times age interaction [$F(2,45) = 3.38, p = 0.043$], but no effect of genotype ($F < 1$) or age [$F(2,45) = 53, p = 0.06$].

Cerebellum

There were significant genotype effect [$F(1,45) = 7.69, p = 0.008$] and genotype \times age interaction [$F(2,45) = 6.54, p = 0.003$], but no age effect ($F < 1$), in L-arginine (Fig. 7a), with higher levels in 4-(32% increase; $p < 0.01$) and 12–14 (20% increase; $p < 0.05$)-month PS19 mice relative to their age-matched WT controls. For L-citrulline (Fig. 7b), we observed significant genotype [$F(1,45) = 4.82, p = 0.03$] and age [$F(2,45) = 6.71, p = 0.0028$] effects and their interaction [$F(2,45) = 13.08, p < 0.0001$], with higher levels in 4-month-old PS19 mice (23% increase; $p < 0.001$). There were no significant genotype and age effects and their interaction in L-ornithine (Fig. 7c) and glutamine (Fig. 7d). A planned comparison, however, revealed higher L-ornithine levels in 4-month PS19 mice relative to their age-matched WT mice (22% increase; $p < 0.05$). For glutamate (Fig. 7e), we found significant age effect [$F(2,45) = 4.59; p = 0.015$] and genotype \times age interaction [$F(2,45) = 18.07, p < 0.0001$], but no genotype effect ($F = 1$), with higher levels in 4-month PS19 mice (22% increase; $p < 0.01$) but lower levels in 8-(11% decrease; $p < 0.05$) and 12–14 (20% decrease; $p < 0.001$)-month-old PS19 mice relative to their age-matched WT controls. Regarding GABA (Fig. 7f), there was a significant genotype \times age interaction [$F(2,45) = 8.03, p = 0.001$], but no genotype or age effect (all $F < 1$), with higher and lower levels in 4-

(24% increase; $p < 0.01$) and 8 (20% decrease; $p < 0.05$)-month PS19 mice, respectively, when compared to their age-matched WT controls. When the glutamine/glutamate ratio was analysed (Fig. 7g), there were no genotype and age effects (all $F < 1$) and their interaction [$F(2,45) = 2.61, p = 0.08$]. A planned comparison, however, revealed a higher ratio in the 12–14-month-old PS19 mice relative to their age-matched WT controls (22% increase; $p < 0.0001$). Regarding the glutamate/GABA ratio (Fig. 7h), we found a significant genotype \times age interaction [$F(2,45) = 3.31, p = 0.046$], but no genotype or age effect (all $F = 1$). For agmatine (Fig. 7i), there was a significant genotype \times age interaction [$F(2,45) = 5.12, p = 0.01$], but no genotype [$F(1,45) = 3.33, p = 0.07$] or age ($F = 1$) effect, with markedly reduced agmatine levels in 4-month PS19 mice when compared with their age-matched WT mice (34% decrease; $p < 0.001$). When putrescine was analysed (Fig. 7j), we found significant effects of genotype [$F(1,45) = 5.97, p = 0.018$], age [$F(2,45) = 3.58, p = 0.036$] and their interaction [$F(2,45) = 6.67, p = 0.003$], with reduced levels in 4 (26% decrease; $p = 0.05$), but increased levels in 8 (85% increase; $p < 0.01$) and 12–14 (39% increase; $p < 0.05$) months, of PS19 mice. Regarding spermidine (Fig. 7k) and spermine (Fig. 7l), there were no significant effects of genotype, age, and their interaction (all $F = 1$).

Discussion

L-Arginine is a versatile amino acid with a number of bioactive metabolites, and polyamines are critically involved in microtubule assembly and stabilization (Savarin et al. 2010; Hamon et al. 2011; Song et al. 2013). Recent research has implicated altered arginine metabolism in the pathogenesis of AD (Inoue et al. 2013; Liu et al. 2014). The present study, for the first time, systematically investigated the time course of the arginine metabolic profile changes in the frontal cortex, hippocampus, parahippocampal region, striatum, thalamus, and cerebellum in PS19 tau mice at 4, 8, and 12–14 months of age. As compared to their wild-type littermates, PS19 mice displayed altered brain arginine metabolism in a region-specific and age-dependent manner.

As illustrated in Fig. 1, L-arginine can be metabolized by NOS, arginase, and ADC to produce L-citrulline (and NO), L-ornithine (and urea), and agmatine, respectively. It has been shown that NOS has an approximately 1000-fold greater affinity for L-arginine than arginase, and endogenous agmatine levels in the mammalian brain are only about 1.5–3.0 nmol per gram of tissue (0.2–0.4 $\mu\text{g/g}$) (Li et al. 1994; Wu and Morris 1998), suggesting the predominance of the NOS pathway under physiological situations. In the present study, PS19 mice displayed significantly increased levels of L-arginine in the hippocampus and cerebellum at 4 (cerebellum) and 12–14 (both regions) months of age, and increased levels of L-citrulline in the cerebellum, but reduced levels in the hippocampus and striatum at 4 and 12–14 months of age, respectively. Argininosuccinate synthetase (ASS) and argininosuccinate lyase (ASL) are responsible for recycling L-citrulline to L-arginine (Fig. 1; Wu and Morris 1998; Wiesinger 2001; Morris 2006). It is currently unclear whether increased L-arginine in the PS19 hippocampus and cerebellum is due to the up-regulation of ASS and ASL. Regarding L-ornithine, interestingly, we observed long-lasting increases in the frontal cortex, hippocampus, and parahippocampal region of PS19 mice at all three age points, although a transient increase in the striatum and cerebellum at 4 months of age. For agmatine, the only significant change observed was reduced levels in the cerebellum of PS19

mice at 4 months of age. While the results demonstrate that MAPT P301S mutation affected multiple metabolic pathways of L-arginine in a region-specific manner, more genotype-related changes in L-ornithine (either long-lasting or transient), however, indicate that the arginase pathway appeared to be affected severely in PS19 mice.

It should be noted that L-citrulline can also be produced from L-ornithine by ornithine transcarbamylase (OTC; Wu and Morris 1998; Wiesinger 2001). OTC, ASS, ASL, and arginase, along with carbamyl phosphate synthetase-I (CPS-I), are the five enzymes of the urea cycle, which dispose of toxic ammonia in the nontoxic and readily excretable form of urea (Morris 2002). The urea cycle is primarily expressed in the liver, and normal brains lack OTC hence do not have a complete urea cycle (Felipo and Butterworth 2002; Wiesinger 2001). Under physiological conditions, brain ammonia is metabolized almost exclusively to glutamine-by-glutamate synthetase (GS) (Wiesinger 2001). Ammonia is produced excessively in the brains of AD patients (Fisman et al. 1985; Seiler 2002). There is evidence suggesting the presence of OTC in AD brains (Bensemain et al. 2009; Cicolini et al. 2016), and the induction of the complete urea cycle perhaps aims to cope with excessive ammonia. As to PS19 mice, it is currently unclear whether the complete urea cycle is present in the brain, and how L-citrulline would be affected. Due to the lack of tissue, unfortunately, the present study was unable to investigate how the activity and/or protein expression of NOS, arginase and other urea cycle enzymes changed in the brain of PS19 mice, which remains to be addressed in future research.

L-Ornithine can be metabolized to glutamate and putrescine via two different pathways (Fig. 1; Wu and Morris 1998). At 4 months of age, PS19 mice displayed increased glutamate levels in the hippocampus and cerebellum, however, with no change or reduced levels in putrescine, suggesting L-ornithine being channelled to glutamate. At this early age point, we also found increased GABA levels and glutamate/GABA ratio (indicating increased neuronal excitability) in the PS19 cerebellum and hippocampus, respectively, which may contribute to the documented early synapse loss and synaptic dysfunction to a certain extent (Yoshiyama et al. 2007). At 8 and 12–14 months of age, interestingly, there were reduced glutamate, but increased putrescine, levels in PS19 mice for all six regions (except for glutamate in the thalamus), indicating an age-related shift of channelling L-ornithine to produce putrescine. Crescenzi et al. (2014) reported reduced glutamate levels in the CA (29%), but not the dentate gyrus, sub-regions of the hippocampus in 20-month PS19 mice using proton magnetic resonance spectroscopy. The present study found a 30% reduction in glutamate in the whole hippocampus of 12–14-month PS19 mice, which appears to be consistent with this earlier report.

Glutamate is considered a downstream metabolite of L-arginine, as L-ornithine can be channelled to produce glutamate (Wu and Morris 1998). It should be noted, however, that in the brain, glutamate can also be synthesized from glutamine by glutaminase in neurons, taken up into astrocytes after released from the synaptic terminals and converted into glutamine by GS, and glutamine is then transported to the neurons and reused to generate glutamate (for a review see Bak et al. 2006). This so-called glutamate–glutamine cycle has been considered to be an important constituent of the glutamatergic neurotransmission system (for a review, see Albrecht et al. 2010). In the present study, there were increased

glutamine/glutamate ratios in 12–14-month-old PS19 mice in the 5 out of 6 brain regions examined, indicating that tau accumulation significantly affects the glutamate–glutamine relationship in the brain with age. Herbrón et al. (2018) produced TauP301L mice with a widespread tau accumulation in the brain by crossbreeding male and female hemizygous rTg4510 mice under the control of prion protein promoter. Interestingly, $^{13}\text{C}/^1\text{H}$ magnetic resonance spectroscopy revealed that TauP301L mice at 2–3 months of age displayed increased glutamate and GABA levels, but decreased glutamine levels, in the brainstem and striatal extracts when compared to the other genotype groups. Moreover, tau expression appeared to affect neuronal–astrocytic metabolism of aspartate, another excitatory amino acid in the central nervous system. These findings demonstrate that tau accumulation in the brain may trigger glutamate toxicity and astrocytic dysfunction in TauP301L mice, which may also apply to PS19 mice. Future research is required to test whether this is the case.

To the best of our knowledge, there is no previous research on polyamines in PS19 mice. As illustrated in Fig. 1, polyamines can be produced by two pathways: de novo synthesis and retro-conversion or catabolic pathways. Putrescine can be produced from L-ornithine by ODC and agmatine by agmatinase, as well as spermidine via the polyamine retro-conversion enzymes spermidine/spermine N-acetyltransferase (SSAT) and polyamine oxidase (PAO) that produce acetylated polyamines (Wallace et al. 2003; Seiller 2004). Spermidine synthase converts putrescine to spermidine, which is then metabolized to spermine by spermine synthase. Spermine can be retro-converted to spermidine by spermine oxidase (SMOX) in addition to SSAT and PAO (Fig. 1). It has been shown that the de novo pathway is the safest way for the production of polyamines, whereas the retro-conversion pathway is the main source of toxic metabolites along with production of polyamines (Seiller 2004). In the present study, PS19 mice at 12–14 months of age displayed increased levels of putrescine in all six brain regions examined, however, accompanied with increased, decreased, or unaltered spermidine and spermine, clearly showing no parallel changes across the three polyamines. Since there were no genotype-related changes in agmatine (in all regions) and spermidine (except for the hippocampus), higher levels of putrescine seen in PS19 mice are likely sourced from L-ornithine via ODC (Fig. 1). However, a systematic investigation is certainly required in the future to fully understand how the de novo synthesis and retro-conversion pathways of polyamines change in the brain of PS19 mice.

Putrescine, spermidine, and spermine are critical for cell proliferation and differentiation, synthesis of DNA, RNA, and proteins, protein phosphorylation, signal transduction, as well as the regulation of neurotransmitter receptors (for reviews, see Williams 1997; Wallace 2000; Oredsson 2003). Polyamines modulate learning and memory by interacting with the polyamine binding site at the NMDA receptors, with spermidine and spermine being the positive modulators and putrescine as a negative influencer (Williams et al. 1991; Rock and Macdonald 1995; Williams 1997). There is evidence suggesting an important role of polyamines (particularly putrescine) in adult neurogenesis (Malaterre et al. 2004). Therefore, the high levels of putrescine in the brain of PS19 mice observed in the present study may have a significant impact on NMDA receptor function and hippocampal neurogenesis, which need to be addressed in future research.

Table 1 summarizes the changes of L-arginine and its downstream metabolites in the six brain regions of PS19 mice at 4, 8, and 12–14 months of age relative to their age-matched wild-type controls. Across the multiple metabolic pathways of L-arginine, the most striking changes were L-ornithine, glutamate, and putrescine, with mild changes in other metabolites in PS19 mice. Regarding the genotype effects in L-ornithine, there were early and persistent increases in the frontal cortex, hippocampus, and parahippocampal region, but transient increases or no change in the striatum, thalamus, and cerebellum. For glutamate, a clear shift from increases or no change at the early age point to decreases at the older age point was seen in five brain regions (except for the thalamus). Regarding putrescine, remarkably, age-related and genotype-specific increases were present in all six brain regions examined. These findings show clearly that the arginine metabolic profile changes in PS19 mice are region-specific with more and consistent changes in the frontal cortex, hippocampus, and parahippocampal region, and very few to a few changes in the thalamus and striatum. The cerebellum is a brain region that contributes to motor control and the procedural aspect of spatial learning (Lalonde and Strazielle 2003; Petrosini 2007). Interestingly, the cerebellum displayed the most of the neurochemical changes (such as increased L-arginine, L-citrulline, L-ornithine glutamate, and GABA levels and decreased agmatine and putrescine levels) in PS19 mice at 4 months of age. These changes may have a significant impact on the cerebellar function and hence contribute to behavioral alterations seen in PS19 mice at 4 months of age (López-González et al. 2015).

In summary, the present study, for the first time, systematically determined the time course of the arginine metabolic profile changes in the frontal cortex, hippocampus, parahippocampal region, striatum, thalamus, and cerebellum in PS19 mice-bearing human MAPT P301S mutation. While the nature of the study is descriptive, the results demonstrate a clear shift of L-arginine metabolism to favor the polyamine production in the brain of PS19 mice along with age-related changes in glutamate, which forms a scientific basis for future research to explore the underlying mechanisms and the functional significance of these changes.

Neuronal microtubules support intracellular transport and neuronal connections, and polyamines are critically involved in microtubule assembly and stabilization (Savarin et al. 2010 ; Hamon et al. 2011; Song et al. 2013) . Accumulation and aggregation of misfolded proteins are hallmarks of neurodegenerative diseases, such as AD, FTD, and prion diseases. Interestingly, spermine increases the acetylation of microtubules (enhancing microtubule stability) and facilitates autophagic degradation of prion aggregates (Phadwal et al. 2018) . Our preliminary work has demonstrated that polyamines (spermine in particular) decrease tau aggregation and promote microtubule assembly (Hunt et al. 2015b). Moreover, sustained arginase I overexpression (hence more L-ornithine and polyamines) reduces tau pathology and mitigates hippocampal atrophy in rTg4510 tau mice (Hunt et al. 2015a). Taken together, we speculate that shifting L-arginine metabolism to favor the polyamine pathway is a protective mechanism aiming to curtail tau pathology. However, there were reduced spermine levels or no change in the brain of PS19 mice, indicating that the system failed to produce more spermine in the presence of high levels of putrescine. Future research will investigate how the enzymes involved in the biosynthesis and retro-conversion of spermine change in the brain of PS19 mice, and explore the preventive and/or therapeutic value of

spermine in tauopathies. Since PS19 mice express P301S mutant tau and model human frontotemporal lobar degeneration (López-González et al. 2015), there is research underway to understand how the brain arginine metabolism changes in FTD patients.

Acknowledgements

This work was supported by the Beth Cobden-Cox Research Grant, and Brain Health Research Centre and Department of Anatomy, University of Otago, New Zealand. The authors would also like to thank the technical staff in the Department of Anatomy and School of Pharmacy, University of Otago, for their assistance. Pranav Vemula is a recipient of the University of Otago Postgraduate Scholarship.

References

- Albrecht J, Sidoryk-W grzynowicz M, Zielińska M, Aschner M (2010) Roles of glutamine in neurotransmission. *Neuron Glia Biol* 6:263–276 [PubMed: 22018046]
- Bae DH, Lane DJR, Jansson PJ, Richardson DR (2018) The old and new biochemistry of polyamines. *Biochim Biophys Acta* 1862:2053–2068
- Bak LK, Schousboe A, Waagepetersen HS (2006) The glutamate/GABA-glutamine cycle: aspects of transport, neurotransmitter homeostasis and ammonia transfer. *J Neurochem* 98:641–653 [PubMed: 16787421]
- Bensemam F, Hot D, Ferreira S, Dumont J, Bombois S, Maurage CA, Huot L, Hermant X, Levillain E, Hubans C, Hansmannel F, Chapuis J, Hauw JJ, Schraen S, Lemoine Y, Buee L, Berr C, Mann D, Pasquier F, Amouyel P, Lambert JC (2009) Evidence for induction of the ornithine transcarbamylase expression in Alzheimer's disease. *Mol Psychiatry* 14:106–116 [PubMed: 17893704]
- Bergin DH, Jing Y, Mockett BG, Zhang H, Abraham WC, Liu P (2018) Altered plasma arginine metabolome precedes behavioural and brain arginine metabolomic profile changes in the APPswe/PS1 E9 mouse model of Alzheimer's disease. *Transl Psychiatry* 8:108 [PubMed: 29802260]
- Burwell RD (2001) Borders and cytoarchitecture of the perirhinal and postrhinal cortices in the rat. *J Comp Neurol* 437:17–41 [PubMed: 11477594]
- Cairns NJ, Bigio EH, Mackenzie IR, Neumann M, Lee VM, Hatanpaa KJ, White CL, 3rd, Schneider JA, Grinberg LT, Halliday G, Duyckaerts C, Lowe JS, Holm IE, Tolnay M, Okamoto K, Yokoo H, Murayama S, Woulfe J, Munoz DG, Dickson DW, Ince PG, Trojanowski JQ, Mann DM (2007) Consortium for frontotemporal lobar degeneration. Neuropathologic diagnostic and nosologic criteria for frontotemporal lobar degeneration: consensus of the Consortium for Frontotemporal Lobar Degeneration. *Acta Neuropathol* 114:5–22 [PubMed: 17579875]
- Calabrese V, Mancuso C, Calvani M, Rizzarelli E, Butterfield DA, Stella AM (2007) Nitric oxide in the central nervous system: neuroprotection versus neurotoxicity. *Nat Rev Neurosci* 8:766–775 [PubMed: 17882254]
- Castellani RJ, Rolston RK, Smith MA (2010) Alzheimer disease. *Dis Mon* 56:484–546 [PubMed: 20831921]
- Cicolini J, Jing Y, Waldvogel HJ, Faull RLM, Liu P (2016) Urea cycle enzymes and peptidylarginine deiminase in Alzheimer's superior frontal gyrus. *Alzheimers Dement* 12:P460
- Crescenzi R, Debrosse C, Nanga RPR, Reddy S, Haris M, Hariharan H, Iba M, Lee VM, Detre JA, Borthakur A (2014) In vivo measurement of glutamate loss is associated with synapse loss in a mouse model of tauopathy. *Neuroimage* 101:185–192 [PubMed: 25003815]
- Esplugues JV (2002) NO as a signalling molecule in the nervous system. *Br J Pharmacol* 135:1079–1095 [PubMed: 11877313]
- Felipo V, Butterworth RF (2002) Neurobiology of ammonia. *Prog Neurobiol* 67:259–279 [PubMed: 12207972]
- Fisman M, Gordon B, Feleki V, Helmes E, Appell J, Rabheru K (1985) Hyperammonemia in Alzheimer's disease. *Am J Psychiatry* 142:71–73 [PubMed: 3966587]
- Gupta N, Jing Y, Collie ND, Zhang H, Liu P (2012) Ageing alters behavioural function and brain arginine metabolism in male Sprague-Dawley rats. *Neuroscience* 226:178–196 [PubMed: 22989918]

- Hamon L, Savarin P, Curmi PA, Pastre D (2011) Rapid assembly and collective behavior of microtubule bundles in the presence of polyamines. *Biophys J* 101:205–216 [PubMed: 21723831]
- Herbrion ML, Javidnia M, Moussa CE (2018) Tau clearance improves astrocytic function and brain glutamate-glutamine cycle. *J Neurol Sci* 391:90–99 [PubMed: 30103978]
- Hortnagl H, Berger ML, Sperk G, Pifl C (1991) Regional heterogeneity in the distribution of neurotransmitter markers in the rat hippocampus. *Neuroscience* 45:261–272 [PubMed: 1684835]
- Hunt JB, Jr, Nash KR, Placides D, Moran P, Selenica ML, Abuqal-been F, Ratnasamy K, Slouha N, Rodriguez-Ospina S, Savlia M, Ranaweera Y, Reid P, Dickey CA, Urcia R, Yang CG, Sandusky LA, Gordon MN, Morgan D, Lee DC (2015a) Sustained arginase 1 expression modulates pathological tau deposits in a mouse model of tauopathy. *J Neurosci* 35:14842–14860 [PubMed: 26538654]
- Hunt JB, Jr, Placides D, Ratnasamy K, Selenica ML, Nash K, Sandusky LA, Abuqalbeen F, Lee DC (2015b) Arginine metabolism and higher-order polyamines impact tau aggregation, microtubule assembly and autophagy in models of tauopathies. *Alzheimers Dement* 11:636–637
- Inoue K, Tsutsui H, Akatsu H, Hashizume Y, Matsukawa N, Yama-moto T, Toyooka T (2013) Metabolic profiling of Alzheimer's disease brains. *Sci Rep* 3:2364 [PubMed: 23917584]
- Irwin DJ, Cairns NJ, Grossman M, Mcmillan CT, Lee EB, Van Deerlin VM, Lee VM, Trojanowski JQ (2015) Frontotemporal lobar degeneration: defining phenotypic diversity through personalized medicine. *Acta Neuropathol* 129:469–491 [PubMed: 25549971]
- Lalonde R, Strazielle C (2003) The effects of cerebellar damage on maze learning in animals. *Cerebellum* 2:300–309 [PubMed: 14964689]
- Leitch B, Shevtsova O, Reusch K, Bergin DH, Liu P (2011) Spatial learning-induced increase in agmatine levels at hippocampal CA1 synapses. *Synapse* 65:146–153 [PubMed: 20572157]
- Li G, Regunathan S, Barrow CJ, Eshraghi J, Cooper R, Reis DJ (1994) Agmatine: an endogenous clonidine-displacing substance in the brain. *Science* 263:966–969 [PubMed: 7906055]
- Liu P, Collie ND, Chary S, Jing Y, Zhang H (2008) Spatial learning results in elevated agmatine levels in the rat brain. *Hippocampus* 18:1094–1098 [PubMed: 18680141]
- Liu P, Jing Y, Collie ND, Chary S, Zhang H (2009) Memory-related changes in L-citrulline and agmatine in the rat brain. *Hippocampus* 19:597–602 [PubMed: 19173225]
- Liu P, Fleete MS, Jing Y, Collie ND, Curtis MA, Waldvogel HJ, Faull RL, Abraham WC, Zhang H (2014) Altered arginine metabolism in Alzheimer's disease brains. *Neurobiol Aging* 35:1992–2003 [PubMed: 24746363]
- Liu P, Jing Y, Collie ND, Dean B, Bilkey DK, Zhang H (2016) Altered brain arginine metabolism in schizophrenia. *Transl Psychiatry* 6:e871 [PubMed: 27529679]
- López-González I, Aso E, Carmona M, Armand-Ugon M, Blanco R, Naudi A, Cabre R, Portero-Otin M, Pamplona R, Ferrer I (2015) Neuroinflammatory gene regulation, mitochondrial function, oxidative stress, and brain lipid modifications with disease progression in tau P301S transgenic mice as a model of frontotemporal lobar degeneration-tau. *J Neuropathol Exp Neurol* 74:975–999 [PubMed: 26360374]
- Malaterre J, Strambi C, Aouane A, Strambi A, Rougon G, Cayre M (2004) A novel role for polyamines in adult neurogenesis in rodent brain. *Eur J Neurosci* 20:317–330 [PubMed: 15233741]
- Morris SM, Jr (2002) Regulation of enzymes of the urea cycle and arginine metabolism. *Annu Rev Nutr* 22:87–105 [PubMed: 12055339]
- Morris SM, Jr (2006) Arginine: beyond protein. *Am J Clin Nutr* 83:508s–512s [PubMed: 16470022]
- Oredsson SM (2003) Polyamine dependence of normal cell-cycle progression. *Biochem Soc Trans* 31:366–370 [PubMed: 12653640]
- Petrosini L (2007) “Do what I do” and “do how I do”: different components of imitative learning are mediated by different neural structures. *Neuroscientist* 13:335–348 [PubMed: 17644765]
- Phadwal K, Kurian D, Salamat MKF, MacRae VE, Diack AB, Manson JC (2018) Spermine increases acetylation of tubulins and facilitates autophagic degradation of prion aggregates. *Sci Rep* 8:10004 [PubMed: 29968775]
- Piletz JE, Aricioglu F, Cheng JT, Fairbanks CA, Gilad VH, Haenisch B, Halaris A, Hong S, Lee JE, Li J, Liu P, Molderings GJ, Rodrigues AL, Satriano J, Seong GJ, Wilcox G, Wu N, Gilad GM (2013)

- Agmatine: clinical applications after 100 years in translation. *Drug Discov Today* 18:880–893 [PubMed: 23769988]
- Reis DJ, Regunathan S (2000) Is agmatine a novel neurotransmitter in brain? *Trends. Pharmacol Sci* 21:187–193 [PubMed: 10785653]
- Rock D, Macdonald R (1995) Polyamine regulation of *N*-methyl-D-aspartate receptor channels. *Annu Rev of Pharmacol Toxicol* 35:463–482 [PubMed: 7598503]
- Rushaidhi M, Jing Y, Zhang H, Liu P (2013) Participation of hippocampal agmatine in spatial learning: an in vivo microdialysis study. *Neuropharmacology* 65:200–205 [PubMed: 23116777]
- Sankaranarayanan S, Barten DM, Vana L, Devidze N, Yang L, Cade-lina G, Hoque N, DeCarr L, Keenan S, Lin A, Cao Y, Snyder B, Zhang B, Nitla M, Hirschfeld G, Barrezueta N, Polson C, Wes P, Rangan VS, Cacace A, Albright CF, Meredith J, Jr, Trojanowski JQ, Lee VM, Brunden KR, Ahljanian M (2015) Passive immunization with phosphotau antibodies reduces tau pathology and functional deficits in two distinct mouse tauopathy models. *PLoS ONE* 10(5):e0125614 [PubMed: 25933020]
- Savarin P, Barbet A, Delga S, Joshi V, Hamon L, Lefevre J, Nakib S, De Bandt JP, Moinard C, Curmi PA, Pastre D (2010) A central role for polyamines in microtubule assembly in cells. *Biochem J* 430:151–159 [PubMed: 20524932]
- Seiler N (2002) Ammonia and Alzheimer's disease. *Neurochem Int* 41:189–207 [PubMed: 12020619]
- Seiller N (2004) Catabolism of polyamines. *Amino Acids* 26:217–233 [PubMed: 15221502]
- Seo S, Liu P, Leitch B (2011) Spatial learning-induced accumulation of agmatine and glutamate at hippocampal CA1 synaptic terminals. *Neuroscience* 192:28–36 [PubMed: 21777660]
- Song Y, Kirkpatrick LL, Schilling AB, Helseth DL, Chabot N, Keillor JW, Johnson GV, Brady ST (2013) Transglutaminase and polyamination of tubulin: posttranslational modification for stabilizing axonal microtubules. *Neuron* 78:109–123 [PubMed: 23583110]
- Wallace HM (2000) The physiological role of the polyamines. *Eur J Clin Invest* 30:72–78 [PubMed: 10620005]
- Wallace HM, Fraser AV, Hughes A (2003) A perspective of polyamine metabolism. *Biochem J* 376:1–14 [PubMed: 13678416]
- Wiesinger H (2001) Arginine metabolism and the synthesis of nitric oxide in the nervous system. *Prog Neurobiol* 64:365–391 [PubMed: 11275358]
- Williams K (1997) Interactions of polyamines with ion channels. *Biochem J* 325:289–297 [PubMed: 9230104]
- Williams K, Romano C, Dichter MA, Molinoff PB (1991) Modulation of the NMDA receptor by polyamines. *Life Sci* 48:469–498 [PubMed: 1825128]
- Wu G, Morris SM (1998) Arginine metabolism: nitric oxide and beyond. *Biochem J* 336:1–17 [PubMed: 9806879]
- Yoshiyama Y, Higuchi M, Zhang B, Huang SM, Iwata N, Saido TC, Maeda J, Suhara T, Trojanowski JQ, Lee VM (2007) Synapse loss and microglial activation precede tangles in a P301S tauopathy mouse model. *Neuron* 53:337–351 [PubMed: 17270732]
- Zhang B, Carroll J, Trojanowski JQ, Yao Y, Iba M, Potuzak JS, Hogan AM, Xie SX, Ballatore C, Smith AB, 3rd, Lee VM, Brunden KR (2012) The microtubule-stabilizing agent, epothilone D, reduces axonal dysfunction, neurotoxicity, cognitive deficits, and Alzheimer-like pathology in an interventional study with aged tau transgenic mice. *J Neurosci* 32:3601–3611 [PubMed: 22423084]
- Zolman JF (1993) *Biostatistics: experimental design and statistical inference* Oxford University Press, Oxford

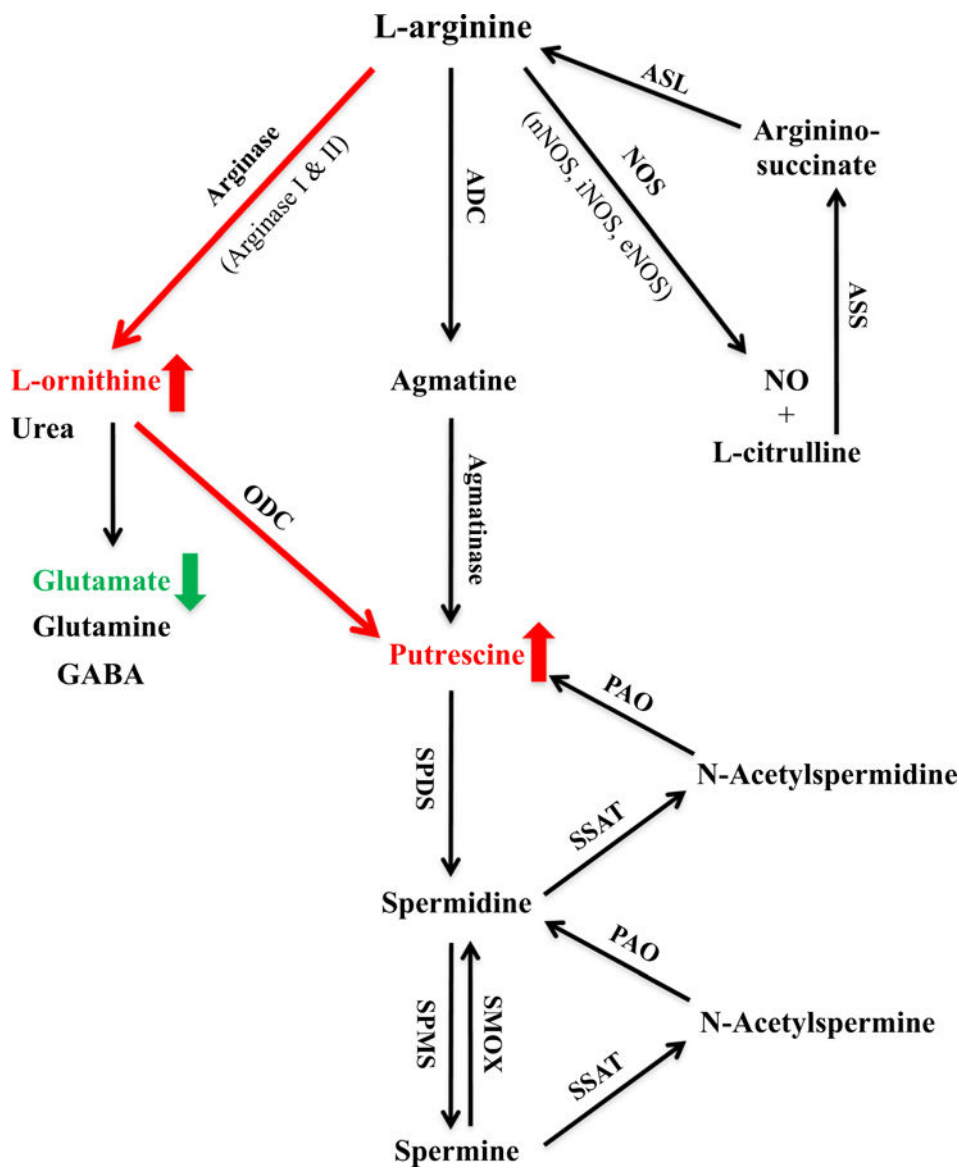


Fig.1.

Arginine metabolic pathways. L-Arginine can be metabolized by nitric oxide synthase (NOS), arginase and arginine decarboxylase (ADC) to form a number of bioactive molecules (see text for detailed description). We found genotype- and age-related increases in L-ornithine and putrescine (indicated by the red letters and short red arrows), but decreases in glutamate (indicated by the green letter and short green arrow) in the brain of PS19 mice, suggesting a shift of arginine metabolism towards the arginase and polyamine system (indicated by the long red arrows). *ASL* argininosuccinate lyase, *ASS* argininosuccinate synthetase, *eNOS* endothelial nitric oxide synthase, *GABA* γ -aminobutyric acid, *iNOS* inducible NOS, *nNOS* neuronal NOS, *NO* nitric oxide, *ODC* ornithine decarboxylase, *PAO* polyamine oxidase, *SMOX* spermine oxidase, *SPDS* spermidine synthase, *SPMS* spermine synthase, *SSAT* spermidine/spermine *N*-acetyltransferase (color figure online)

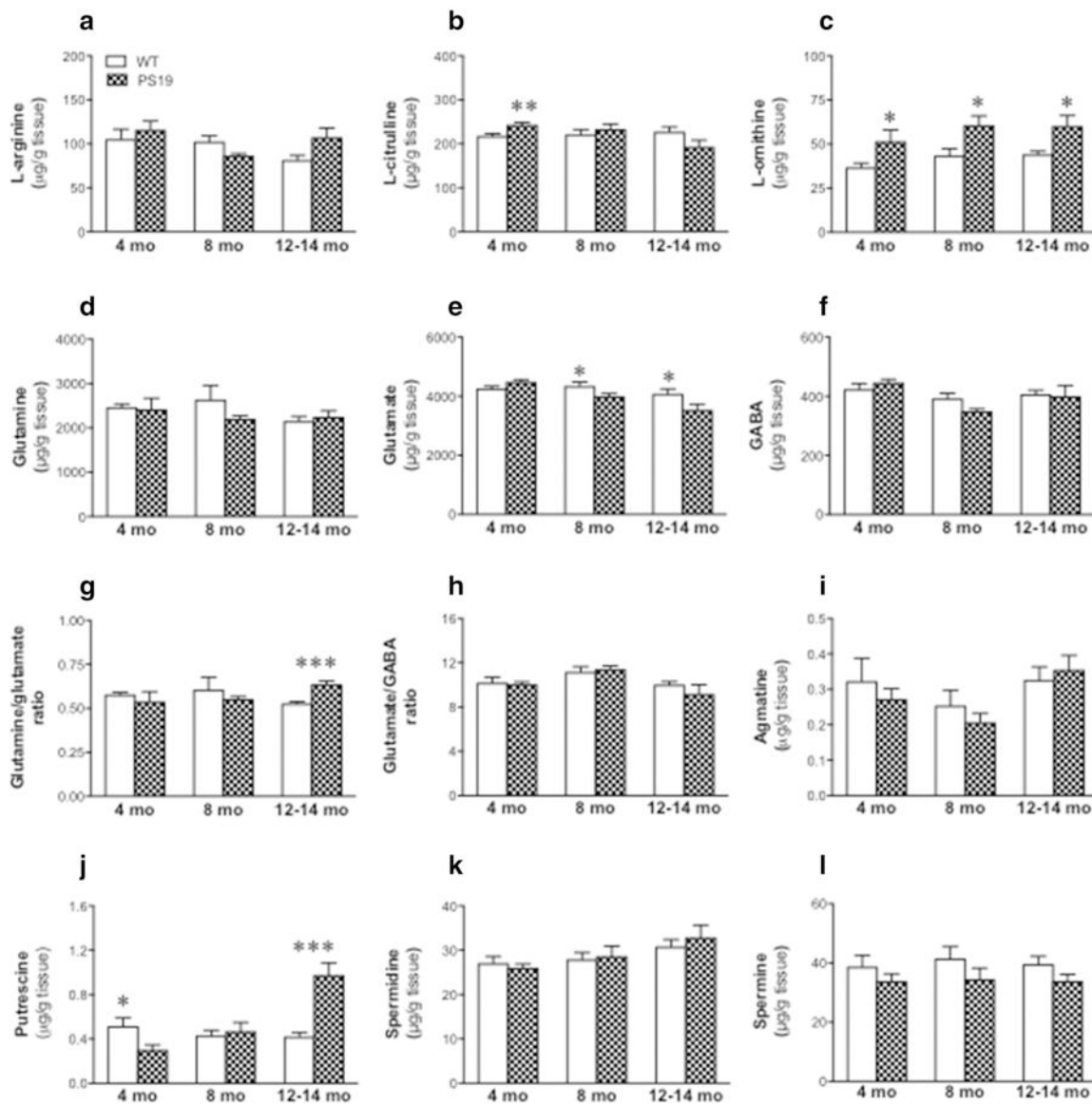


Fig.2. Mean (± SEM) levels of L-arginine (a), L-citrulline (b), L-ornithine (c), glutamine (d), glutamate (e), GABA (f), glutamine/glutamate ratio (g), glutamate/GABA ratio (h), agmatine (i), putrescine (j), spermidine (k), and spermine (l) in the frontal cortex from the wild-type and PS19 mice at 4, 8, and 12–14 months of age (*n* = 8–11/genotype/age). Asterisks indicate significant differences between groups at **p* < 0.05 or ****p* < 0.001

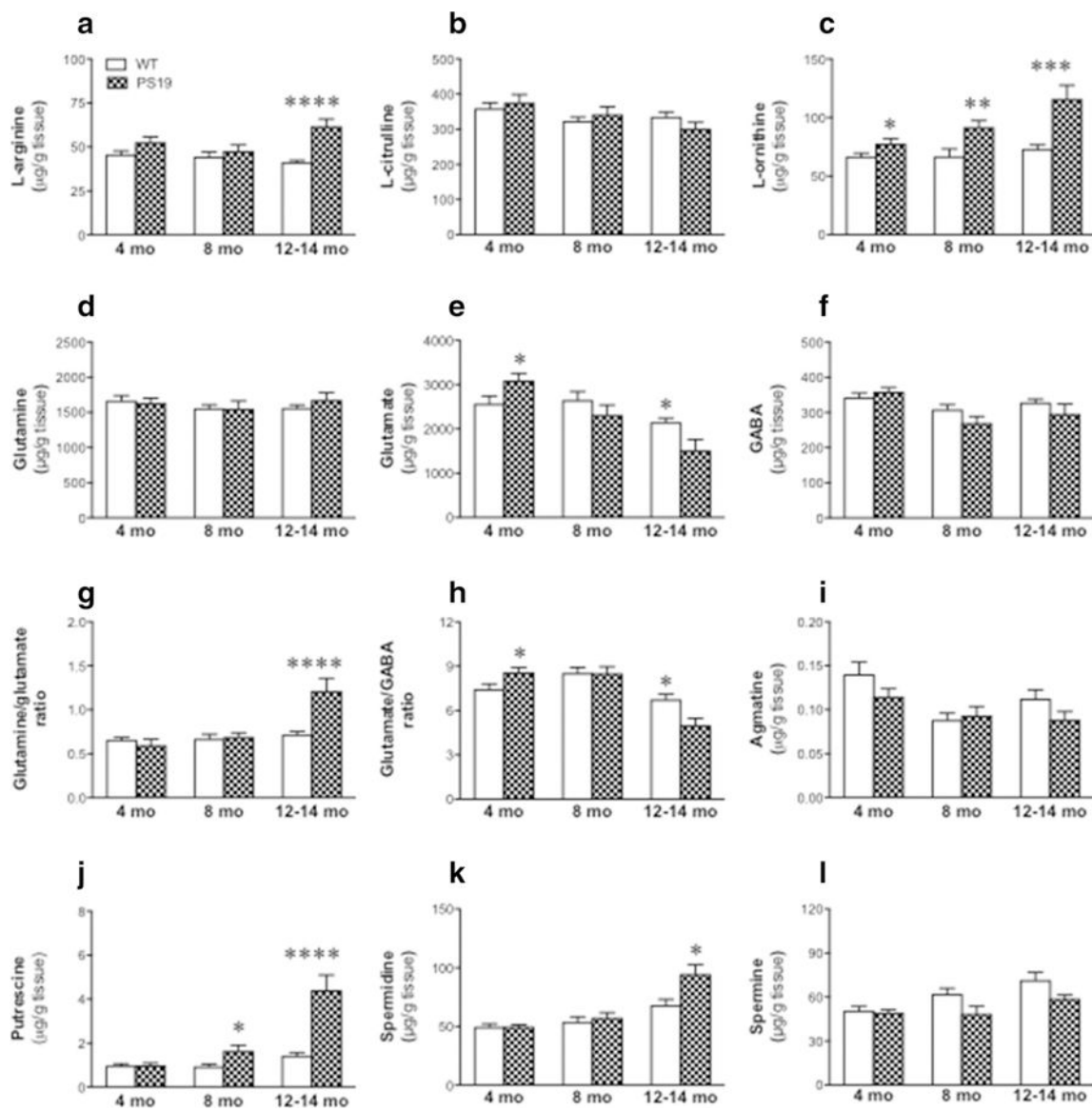


Fig.3. Mean (\pm SEM) levels of L-arginine (a), L-citrulline (b), L-ornithine (c), glutamine (d), glutamate (e), GABA (f), glutamine/glutamate ratio (g), glutamate/GABA ratio (h), agmatine (i), putrescine (j), spermidine (k), and spermine (l) in the hippocampus from the wild-type and PS19 mice at 4, 8, and 12–14 months of age ($n = 8–11/\text{genotype}/\text{age}$). Asterisks indicate significant differences between groups at * $p < 0.05$, ** $p < 0.01$, *** $p < 0.001$, or **** $p < 0.0001$

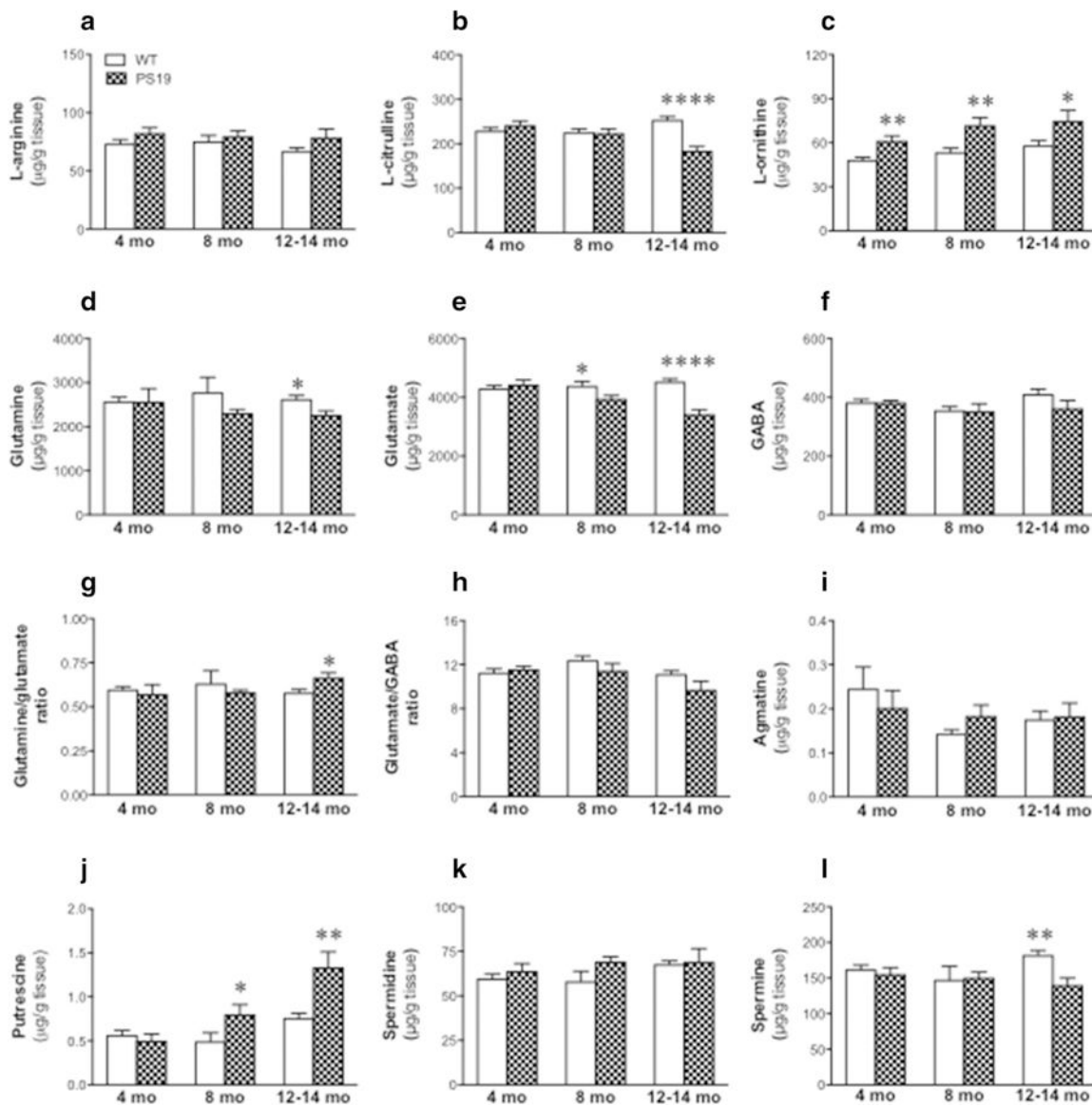


Fig.4. Mean (\pm SEM) levels of L-arginine (a), L-citrulline (b), L-ornithine (c), glutamine (d), glutamate (e), GABA (f), glutamine/glutamate ratio (g), glutamate/GABA ratio (h), agmatine (i), putrescine (j), spermidine (k), and spermine (l) in the parahippocampal region from the wild-type and PS19 mice at 4, 8, and 12–14 months of age ($n = 8–11/\text{genotype}/\text{age}$). Asterisks indicate significant differences between groups at * $p < 0.05$, ** $p < 0.01$, or **** $p < 0.0001$

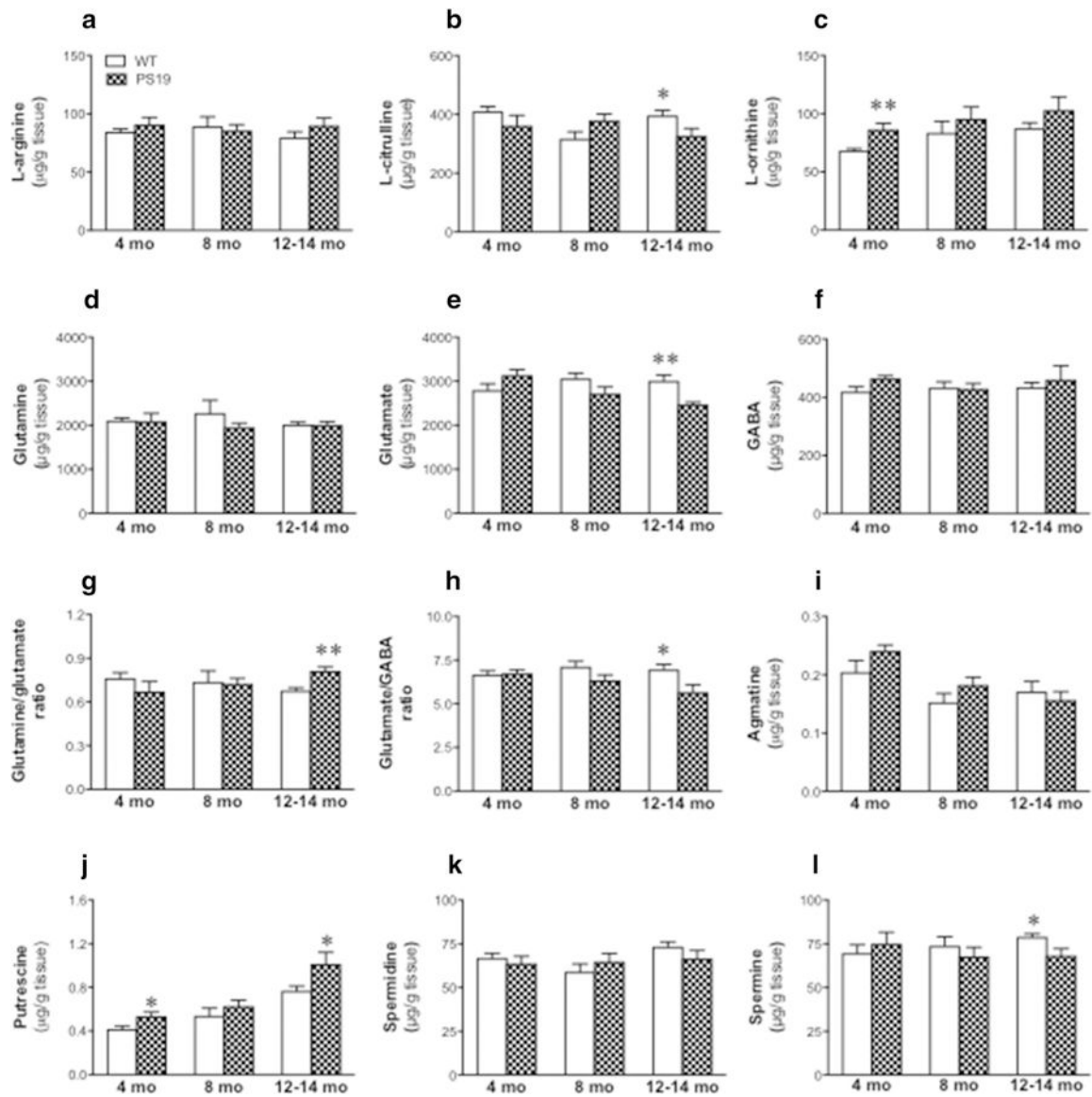


Fig.5. Mean (\pm SEM) levels of L-arginine (a), L-citrulline (b), L-ornithine (c), glutamine (d), glutamate (e), GABA (f), glutamine/glutamate ratio (g), glutamate/GABA ratio (h), agmatine (i), putrescine (j), spermidine (k), and spermine (l) in the striatum from the wild-type and PS19 mice at 4, 8, and 12–14 months of age ($n = 8–11/\text{genotype/age}$). Asterisks indicate significant differences between groups at * $p < 0.05$, ** $p < 0.01$

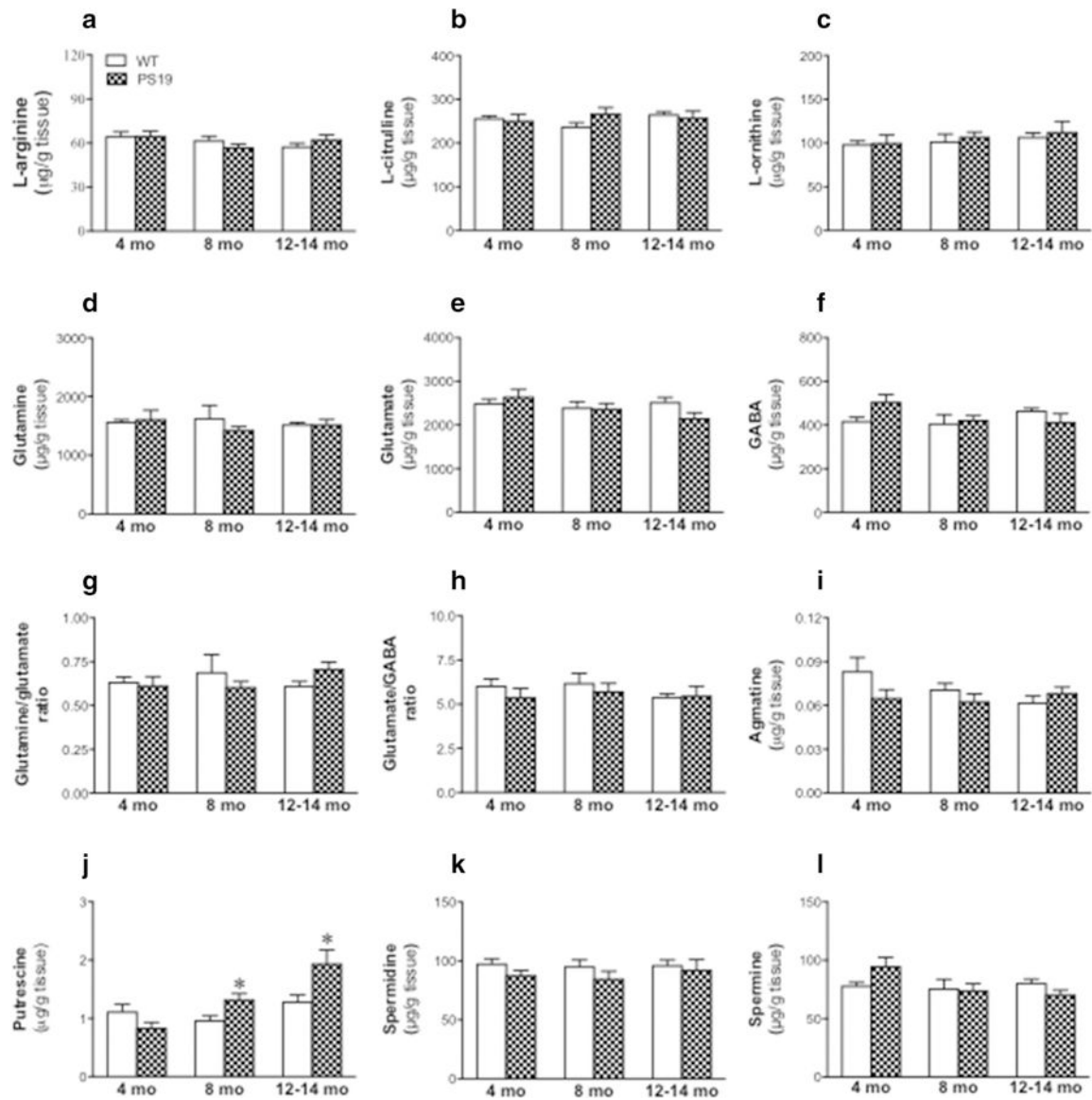


Fig.6. Mean (\pm SEM) levels of L-arginine (a), L-citrulline (b), L-ornithine (c), glutamine (d), glutamate (e), GABA (f), glutamine/glutamate ratio (g), glutamate/GABA ratio (h), agmatine (i), putrescine (j), spermidine (k), and spermine (l) in the thalamus from the wild-type and PS19 mice at 4, 8, and 12–14 months of age ($n = 8–11/\text{genotype/age}$). Asterisks indicate significant differences between groups at $*p < 0.05$

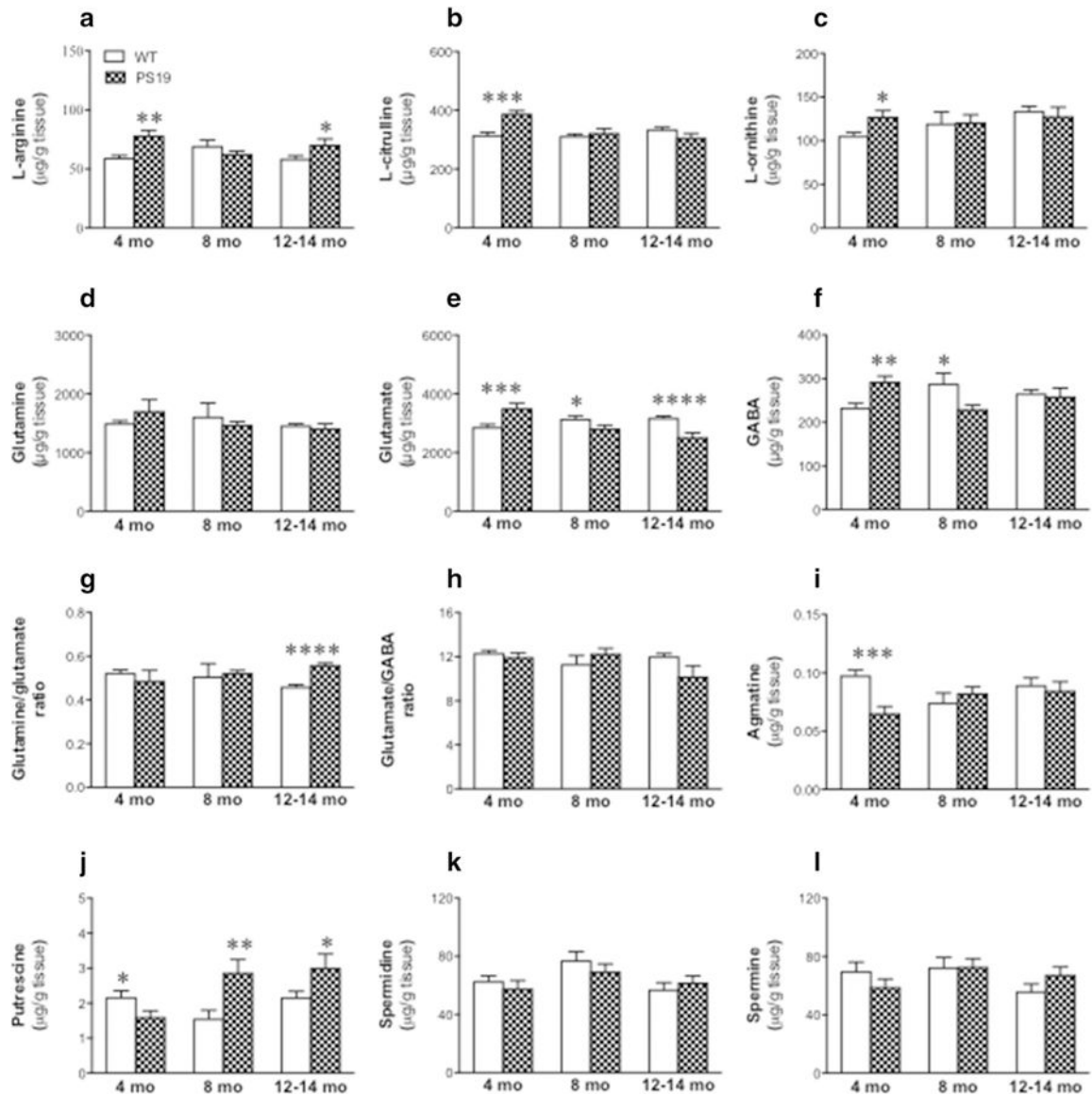


Fig.7. Mean (\pm SEM) levels of L-arginine (a), L-citrulline (b), L-ornithine (c), glutamine (d), glutamate (e), GABA (f), glutamine/glutamate ratio (g), glutamate/GABA ratio (h), agmatine (i), putrescine (j), spermidine (k), and spermine (l) in the cerebellum from the wild-type and PS19 mice at 4, 8, and 12–14 months of age ($n = 8–11/\text{genotype}/\text{age}$). Asterisks indicate significant differences between groups at * $p < 0.05$, ** $p < 0.01$, *** $p < 0.001$, or **** $p < 0.0001$

Table 1

Summary of the neurochemical changes in PS19 mice relative to WT mice

Brain regions	Age (months)	ARG	CIT	ORN	GLN	GLUT	GABA	GLN/GLUT	GLUT/GABA	AGM	PUT	SPD	SPM
Frontal cortex	4	-	-	↑	-	-	-	-	-	-	↓	-	-
	8	-	-	↑	-	↓	-	-	-	-	-	-	-
	12-14	-	-	↑	-	↓	-	↑	-	-	↑	-	-
Hippocampus	4	-	-	↑	-	↑	-	-	↑	-	-	-	-
	8	-	-	↑	-	-	-	-	-	-	↑	-	-
	12-14	↑	-	↑	-	↓	-	↑	↓	-	↑	↑	-
Parahippocampal region	4	-	-	↑	-	-	-	-	-	-	-	-	-
	8	-	-	↑	-	↓	-	-	-	-	↑	-	-
	12-14	-	↓	↑	↓	↓	-	↑	-	-	↑	-	↓
Striatum	4	-	-	↑	-	-	-	-	-	-	↑	-	-
	8	-	-	-	-	-	-	-	-	-	-	-	-
	12-14	-	↓	-	-	↓	-	↑	↓	-	↑	-	↓
Thalamus	4	-	-	-	-	-	-	-	-	-	-	-	-
	8	-	-	-	-	-	-	-	-	-	↑	-	-
	12-14	-	-	-	-	-	-	-	-	-	↑	-	-
Cerebellum	4	↑	↑	↑	-	↑	↑	-	-	↓	↓	-	-
	8	-	-	-	-	↓	↓	-	-	-	↑	-	-
	12-14	↑	-	-	-	↓	-	↑	-	-	↑	-	-

AGM Agmatine, ARG Arginine, CITL-citrulline, GABA γ -aminobutyric acid, GLN glutamine, GLN/GLUT glutamine/glutamate ratio, GLUT/GABA glutamate/GABA ratio, ORNL-ornithine, PUT putrescine, SPD spermidine, SPM spermine